

One-dimensional experimental study of rainfall infiltration into unsaturated soil



Estudio experimental unidimensional de la infiltración de lluvia en suelos parcialmente saturados

Juan David Montoya-Dominguez¹, Edwin Fabián García-Aristizábal², Carlos Alberto Vega-Posada^{2*}

¹Geomecánica Integral S.A.S. Transversal 32 C sur # 32 B -03. C. P. 055422. Envigado, Colombia.

²Facultad de Ingeniería, Universidad de Antioquia. Calle 67 # 53-108. A. A. 1226. Medellín, Colombia.

ARTICLE INFO

Received July 17, 2016

Accepted February 13, 2017

KEYWORDS

Unsaturated soil, initial water content, water infiltration, laboratory testing, one-dimensional infiltration

Suelo parcialmente saturado, contenido inicial de agua, infiltración de agua, ensayos de laboratorio, infiltración unidimensional

ABSTRACT: This paper presents experimental results obtained from tests on unsaturated soil in one-dimensional columns simulating a rainfall infiltration process. Six columns composed of compacted Silty Sand were prepared to study the effects of the initial water content and rainfall intensity on the downward infiltration process. The advance of the water front was monitored using sensors to measure pore water pressure and volumetric water content installed at different locations along the height of the Silty Sand column. The test results show that the lag time, defined as the time difference from the beginning of the test to a sudden increase in the volumetric water content readings, was influenced by the soil initial water content and rainfall intensity; it is observed that the lag time is shorter at higher initial water contents and greater rainfall intensities. The results provide insights to understand the hydraulic behavior of unsaturated slopes and embankments exposed to rainfall infiltration.

RESUMEN: En este artículo se presentan los resultados experimentales obtenidos a partir de ensayos en suelo parcialmente saturado en columnas unidimensionales, simulando un proceso de infiltración de lluvia. Se prepararon seis columnas de arena limosa compactada para estudiar los efectos del contenido inicial de agua y de la intensidad de la lluvia en el proceso de infiltración descendente. El avance del agua fue monitoreado usando sensores para medir la presión de poros y de contenido volumétrico de agua instalados a diferentes alturas de la columna de arena limosa. Los resultados de los ensayos muestran que el tiempo de retraso, definido como la diferencia de tiempo desde el inicio del ensayo hasta el aumento súbito en las lecturas del contenido volumétrico de agua, fue influenciado por el contenido inicial de agua en el suelo y la intensidad de la lluvia; se observa que el tiempo de retraso es más corto a mayores contenidos iniciales de agua y mayores intensidades de lluvia. Estos resultados proveen información para comprender el comportamiento hidráulico de taludes y terraplenes parcialmente saturados expuestos a la infiltración de lluvias.

1. Introduction

Infiltration through an unsaturated soil is generally assumed to be the result of precipitation or surface processes that involve the use of water. The dynamic of such processes is mainly controlled by capillary and gravity forces, and for most practical problems is formulated as a one-dimensional flow in the vertical direction [1]. Additionally, the infiltration process is generally conceptualized as occurring in three stages: infiltration, redistribution, and drainage [2].

Understanding the different factors (e.g. effects of initial water content, rainfall intensity, rainfall duration, saturation-suction relationships, saturation-permeability relationships, etc.) that influence the water movement

through an unsaturated soil, has been a subject of interest to many professionals such as hydrologist, geologist, soil scientists, geotechnical, environmental, agriculture engineers, etc. [3-5]. This knowledge is crucial to understand soil behavior related to runoff prediction due to heavy rainfall, erosion, sediment transport and flooding control, rainfall induced landslides, estimation of aquifers recharge, estimation of water availability for plants, contaminants travel velocity, etc.

One-dimensional water infiltration into unsaturated soils has been studied from different points of view. For instance, [6-8] used analytical solutions to study the effect of hydraulic parameters and rainfall conditions on the infiltration of unsaturated homogeneous and two-layered soils. These studies showed the influence of the hydrology and hydraulic parameters of the materials on changes on the pore water pressures and volumetric strains. Recently, numerical solutions have emerged as a need to analyze the complexity of the initial and boundary condition, multiple soil layers, variable geometries and rainfall conditions of engineering problems that are not considered by analytical

* Corresponding author: Carlos Alberto Vega Posada

e-mail: carlosa.vega@udea.edu.co

ISSN 0120-6230

e-ISSN 2422-2844



methods [9-14]. On the other hand, some researchers have performed experimental studies to understand the one-dimensional infiltration process into unsaturated geomaterials [15-17]. These investigations have focused mainly on assessing the variables affecting infiltration, and the hydraulic interaction of soils and soil-geosynthetics systems. Although, analytical and numerical solutions allow the study of more complex problems, experimental studies are still necessary to fully understand the rainfall infiltration process on unsaturated soils. Additionally, the data collected from experimental programs are a valuable source of information useful to calibrate models and to conduct computational calculations.

This paper studies the effects of the soil initial water content and rainfall intensity on the downward infiltration process into an unsaturated sand. Six columns composed of compacted silty sand were prepared and tested for this purpose. Because the rainfall infiltration throughout an unsaturated zone is predominantly downward, the results presented herein can also be used to understand the hydraulic response of unsaturated slopes and embankments subjected to a rainfall. From the results, it is observed that the time between rainfall infiltration and the arrival of the wetting front, lag time, is strongly affected by the initial volumetric water content and rainfall intensity. The results provide insights to understand the hydraulics and dynamics of infiltration processes throughout unsaturated geomaterials.

2. Laboratory experimental program

2.1. Materials

A soil known as Edosaki sand was used to conduct the experiments. The physical properties of the soil are listed in Table 1. The grain size distribution curve was obtained by a sieve analysis and it is presented on Figure 1(a). This soil was classified as silty sand (SM), according to the Unified Soil Classification System (USCS) [18]. Figure 1(b) shows the soil water characteristic curve (SWCC) obtained using

Tempe Pressure cell. The experimental data was fitted, for the wetting and drying paths, using Van Genuchten Equation [19]. Details about measurement of physical parameters and SWCC can be obtained from [20].

Table 1 Material parameters of Edosaki sand

Material parameter	Silty sand
Specific gravity - G_s	2.75
Mean grain size - D_{50} (mm)	0.23
Coefficient of uniformity - C_u	16.67
Coefficient of gradation - C_c	4.70
Fines content - (%)	16.40
Plastic index	No plastic
Void ratio e_{max}/e_{min}	1.59/1.01
Max. Dry unit weight - γ_d (kN/m ³)	17.20
Optimum moisture content - w_{opt} (%)	16.01

2.2. Equipment and instrumentation set-up

Figure 2 shows a sketch of the sand column and the location of the sensors used to measure the advance of the wetting front. The major components of the system are: acrylic cylinder, pore water pressure sensors, ceramic cups, water content sensors, and rainfall system. The acrylic columns were instrumented with pore water pressure and moisture content sensors located at 5, 15 and 25 cm from the bottom of the sand column.

Sand columns were prepared by using the wet tamping method, and with an average dry unit weight of 12 kN/m³. The construction procedure is described as follows: A gravel layer of 1 cm thickness was placed at the bottom of the acrylic cylinder and covered with a non-woven geotextile. Then, the sand was mixed to reach a target initial water content and deposited on multiple layers over the geotextile. Each layer was tamped to reach the target dry unit weight, as shown in Figure 3. Three holes were drilled on the cylinder's wall to locate the pore water pressure (PWP) sensors at three

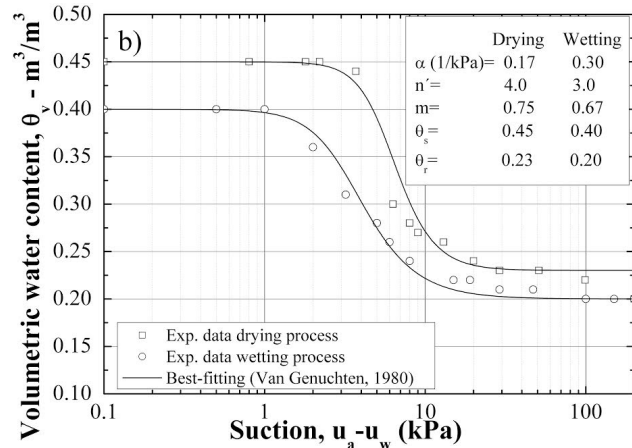
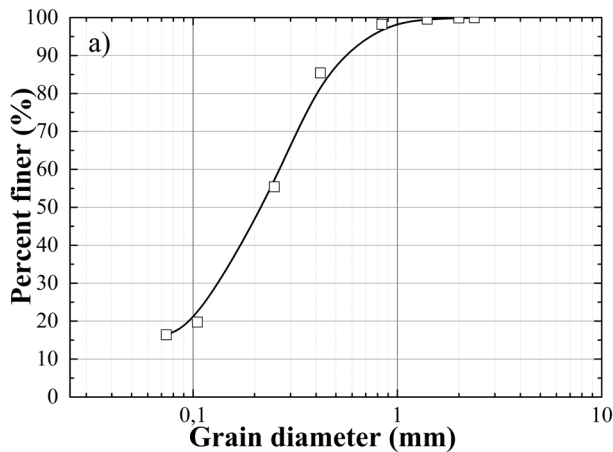


Figure 1 a) Grain size distribution curve, b) Soil Water Characteristic Curve

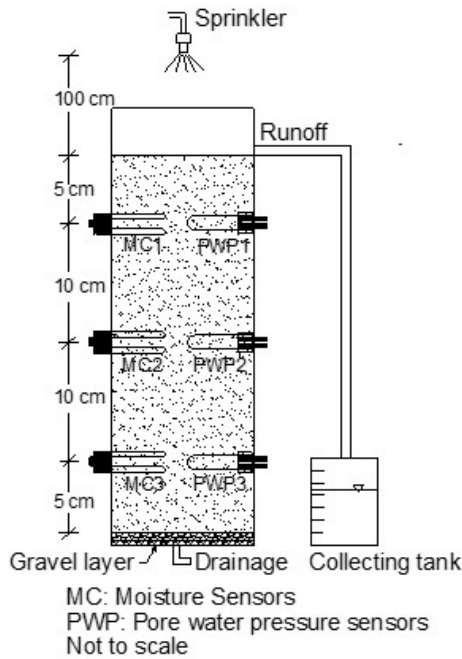


Figure 2 Sketch of the one-dimensional column test and location of the sensors

selected heights, as sketched in Figure 2. The Moisture content (MC) sensors were installed after completion of the sand column by inserting the probes at the same heights of the PWP sensors. Finally, a small acrylic tank was connected at the bottom of the sand column to collect the water drained at the base, and another one connected at the top to collect the runoff water. A sprinkler connected to the water supply and placed 100 cm above the sand column surface was used as the rainfall simulator system (Figure 4(a)).

PWP transducers were used to monitor the negative pore water pressure change induced by the infiltration of the water. A porous ceramic with a round bottom straight cup was attached to the transducers to measure negative pore water pressures. The porous ceramic had an air entry value of 100 kPa and measured 1.27 cm in diameter, 6.35 cm in length and 0.32 cm in thickness. The soil moisture transducers (ECH20 EC-5) were used to monitor the volumetric water content. Both, pore water pressure and moisture content sensors are shown in Figure 4(b). The output signals from the electronic transducers were sent to an A/D converter and then to the data logger, where

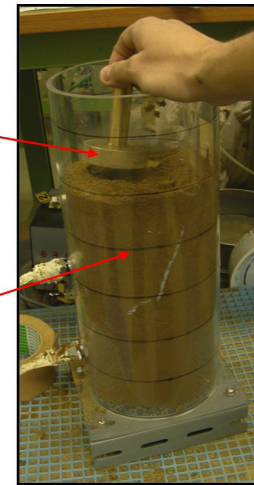


Figure 3 Compaction process for preparation of the sand columns

data sampling were recorded for the wetting and drying processes.

2.3. Procedures

In total, six sand column tests were performed. Table 2 shows the main parameters of the testing program. The infiltration process was analyzed by applying an artificial rainfall to the sand columns. The sand columns were prepared at various initial water contents, and then subjected to rainfall intensities varying from 50 to 75 mm/h. The rainfall intensity was controlled by adjusting a water pressure regulator located between the water supply and the sprinkler. Rainfall was applied as homogeneously as possible on an area of approximately 1.5 m² and measured using a burette. Cumulative rainfall was recorded at different time intervals during the testing procedure, and the rainfall intensity was calculated as the gradient of the cumulative rainfall versus time. Excess of water on the surface was collected on a tank.

3. Results and discussion

3.1. Pore water pressure readings

Figure 5 shows a typical response of the PWP sensors (test CT-01) to the induced artificial rainfall event. It can be observed that the negative pore water pressure (suction)

Table 2 General information of the column test

Test No.	Optimum water content (%)	Unit weight of dry soil (kN/m ³)	Rainfall intensity (mm/h)	Duration (s)
CT-01	16.01	12.00	75.2	2890
CT-02			50.6	5450
CT-03			68.2	5415
CT-04			74.4	3830
CT-05			52.8	8995
CT-06			61.1	7345

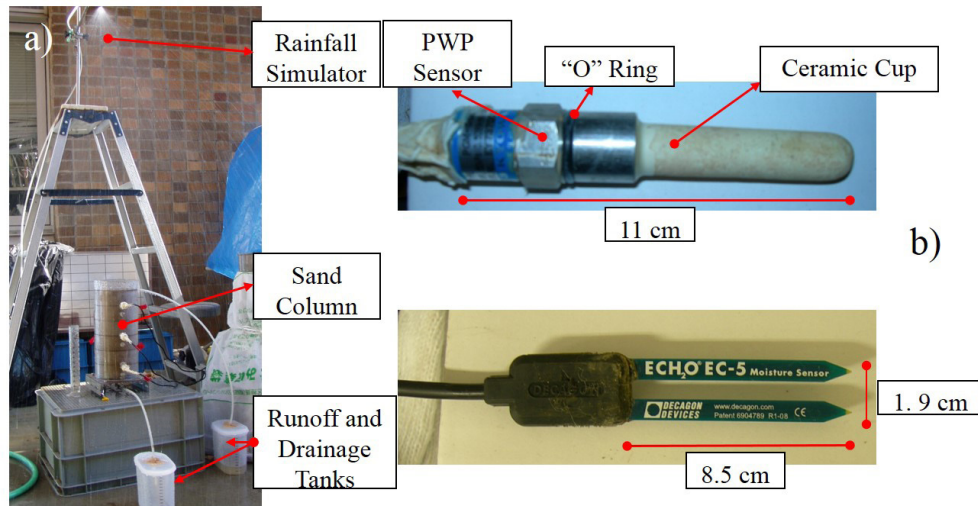


Figure 4 a) Setup for the experiment and rainfall system, b) Pore water pressure and water content sensors

is reduced, indicating that the wetting front reached the sensors' location. The first sensor to respond was PWP1, followed by PWP2 and PWP3, respectively. The time lag between the sensors indicates the velocity of advance of the wetting front.

The change in negative pore water pressure within the soil is strongly related to depth. Sensor PWP1 recorded larger negative pore water pressure than PWP2, and PWP2 larger negative pressures than PWP3. This response is explained by the accumulation of water from the bottom to the top of the sand column, due to the rainfall infiltration.

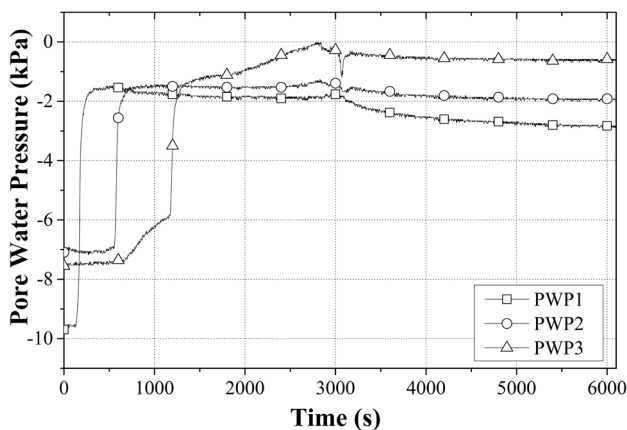


Figure 5 Typical pore water pressure response (CT-01)

3.2. Volumetric water content readings

The infiltration response of the column tests was analyzed by interpreting the data recorded by the Volumetric water content (VWC) sensors. Figure 6 show the response of the moisture water content sensors located at depths of 5, 15 and 25 cm, respectively. From Figure 6(a), it can be observed that, although the initial water content was different from all column tests, the maximum water content value

recorded by the MC sensors during the infiltration process was similar (22-24%). In addition, the moisture contents followed almost the same trend and approached to the same residual value during the last stage of the drainage process. Similar trends were captured for the sensors located at depths of 15 and 25 cm, where the maximum water content values recorded were 25-30% and 30-35%, respectively. These last two water content histories are presented in Figures 6(b) and 6(c), respectively.

According to the results presented in Figure 6, the infiltration process throughout an unsaturated sand column can be described in four steps. These steps are schematically shown in Figure 7 and can be described by means of the measured moisture contents during the rainfall infiltration processes as follows:

Step 1

Initial volumetric water content (IWC). It is the volumetric water content of the soil at each location of the MC sensors, just before rainfall starts. Initial water contents at the MC sensors are listed in Table 3.

Step 2

Lag Time. Corresponds to the time difference from the beginning of the test to a sudden increase in the volumetric water content readings. The lag time reflects how fast the water front moves through an unsaturated soil at the early stage of the infiltration process, and can be useful to estimate the time when the wetting front will reach a specific location of the soil's profile. The lag time was measured directly from the moisture content readings and are presented in Table 4. This table also presents the rainfall intensity and duration applied to each sand column.

Step 3

Maximum water content. Corresponds to the maximum volumetric water content that can be achieved at each

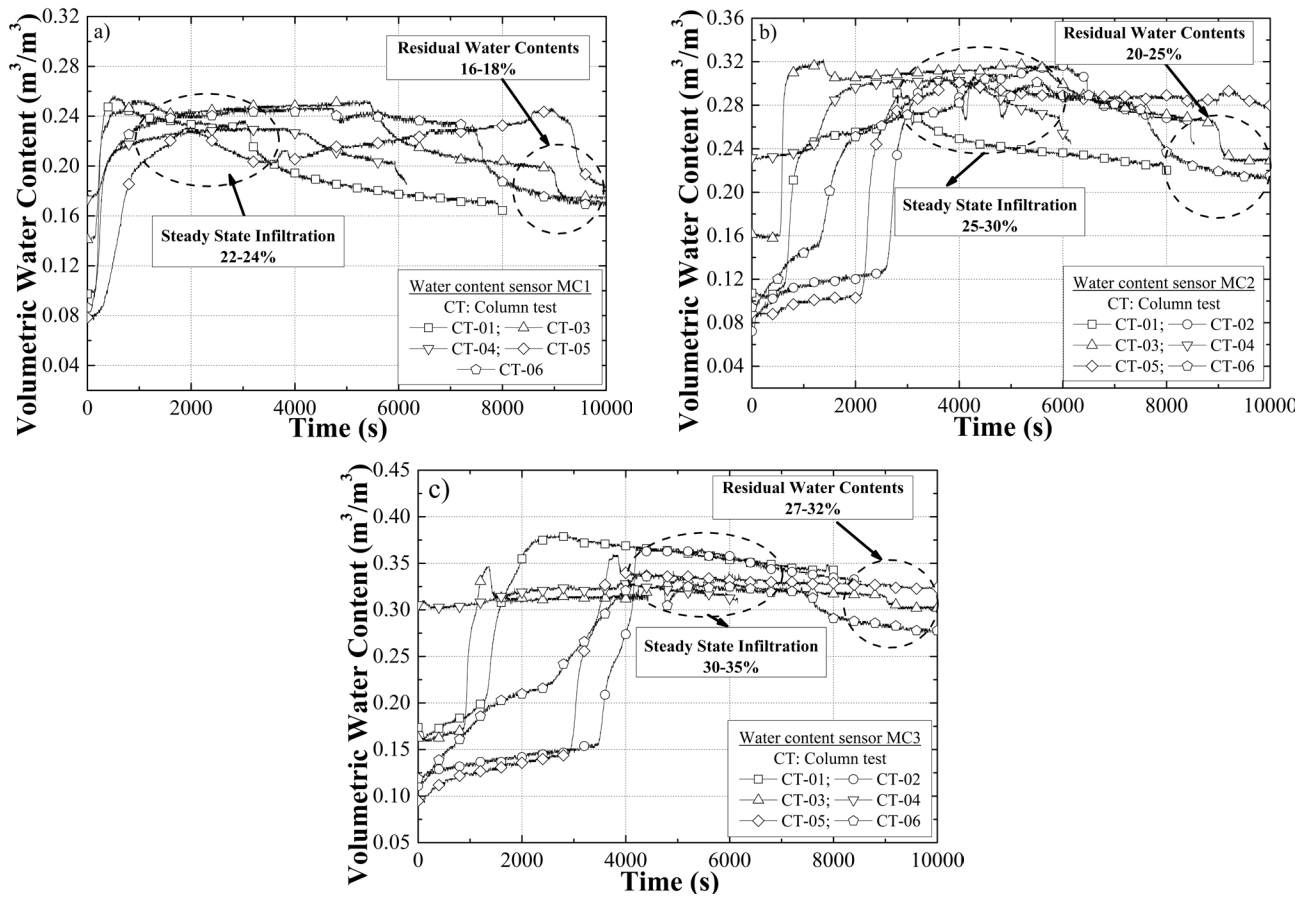


Figure 6 Moisture content responses recorded by a) sensor MC1, b) sensor MC2, and c) Sensor MC3

Table 3 Initial volumetric water contents measured by the MC sensors

Test No.	Initial volumetric water content – IWC (%)		
	Distance from the sand surface		
	5 cm	15 cm	25 cm
CT-01	9.7	10.7	17.2
CT-02	5.2	7.3	11.2
CT-03	14.1	15.9	16.1
CT-04	17.4	22.9	30.4
CT-05	7.9	8.9	9.6
CT-06	8.4	9.5	11.0

Table 4 Time lag measurement from MC reading, rainfall intensity and duration

Test No.	Time lag (s)			Rainfall (mm/h)	Duration (s)
	Distance from the sand surface				
	5 cm	15 cm	25 cm		
CT-01	131	635	1336	75.2	2890
CT-02	698	2501	3527	50.6	5450
CT-03	124	503	862	68.2	5415
CT-04	73	440	892	74.4	3830
CT-05	259	2116	2980	52.8	8995
CT-06	144	1274	2510	61.1	7345

location within the soil profile; it is reached when the maximum saturations are approached. At this stage, the infiltration rate decreases and the volumetric water contents are closed to be constant during the rainfall event. Figure 6 show the maximum water contents at each location of the MC sensors. Table 5 summarizes these results.

Table 5 Maximum water contents measured by the MC sensors

Depth (cm)	Volumetric water content (%)
5	22-24
15	25-30
25	30-35

Step 4

Drainage. When rainfall stops, the water is drained out to start with the drying cycle. After equilibrium is achieved, a residual water content, greater than the initial water content, remains stored in the sand column. In that sense, the drainage curve can be useful to predict the residual volumetric water content stored in the soil immediately after a rainfall event. Figure 6 show the residual water contents for the sand column tested. In addition, it is observed that after rainfall stops, the bottom of the sand column had a larger water content than that measured at the surface. This response is explained by the drying process, which starts first at the top of the column and finishes at the bottom. The residual volumetric water contents are summarized in Table 6.

Table 6 Residual water contents measured by the MC sensors

Depth (cm)	Volumetric water content (%)
5	16-18
15	20-25
25	27-32

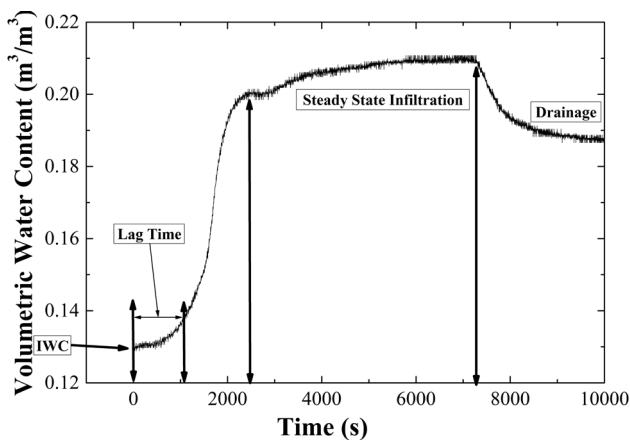


Figure 7 Stages of the moisture content time histories

3.3. Effect of initial volumetric water content on the infiltration process

Six sand columns were constructed with different initial water contents and subjected to an infiltration process. In this section, the early stage of the infiltration process is analyzed by considering the effects of the initial water content on the elapsed time between the beginning of the rainfall infiltration and the arrival of the wetting front to the MC sensors. The relationship between the initial volumetric water content measured at the MC sensors, presented in Table 3, and the lag time for infiltration, presented in Table 4, are plotted in Figure 8.

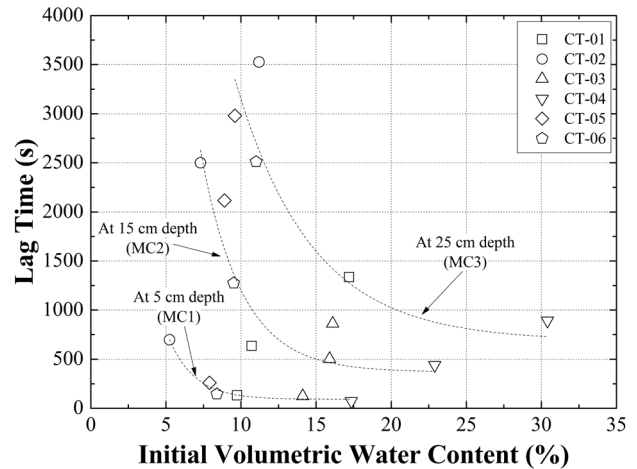


Figure 8 Initial water content vs. lag time

From Figure 8, it can be observed how the lag time is controlled by the initial volumetric water content. In other words, the time between rainfall initiation and the arrival of the wetting front is dependent on the soil initial volumetric water content. At a depth of 5 cm, the test with the lowest initial water content (CT-02, $\theta_w=5.2\%$) exhibited the longest lag time ($t=698s$), while the test with the highest initial water content (CT-04 $\theta_w=17.4\%$) exhibited the shortest lag time ($t=73s$). A similar behavior was observed for the sensor located at a depth of 15 cm, where the test with lowest initial water content (CT-02, $\theta_w=7.3\%$) had a lag time of 2501s, and the one with the highest initial water content (CT-04 $\theta_w=22.9\%$) had a lag time of 440 s. At 25 cm depth, the readings followed the same general trend. The results suggest that, the higher the initial volumetric water content the shorter the lag time, meaning that the infiltration process is faster and the water reaches sooner the deeper soil.

Water movement through an unsaturated soil during the wetting and drying cycles is governed by the water content and matric suction (i.e. negative pore water pressure); the lower the water content, the greater the suction, and consequently it is more tortuous for the water to move along the soil skeleton. This fact can be the reason why the initial water contents and lag time showed an inverse relation during the tests. Lag times reflect how fast the water moves through an unsaturated soil at the early stage

of the infiltration process and can be useful to predict the time when the wetting front will reach a specific location in the soil profile, by considering the effects of the initial volumetric water content and rainfall intensity.

3.4. Effect of rainfall intensity on the infiltration process

Each of the sand columns was subjected to a rainfall intensity applied at a constant rate (mm/h). In this section, the early stage of the infiltration process was analyzed by considering the effects of rainfall intensity on the elapsed time between rainfall initiation and the wetting front arrival. Figure 9 shows the relationship between rainfall intensity and lag time as registered by the MC sensors located at depths of 5, 15 and 25 cm. These results show, regardless of the sensor location, a similar trend at all depths; which is that, the wetting front reaches faster the different locations on the sand column as the intensity of rainfall increases.

These observations suggest that the rainfall intensity has a markedly influence on the unsaturated infiltration process. One plausible explanation could be the rising of soil saturation (i.e., reduction of suction) and the unsaturated permeability as a consequence of the increment of water flux at the soil surface, when rainfall intensity is higher.

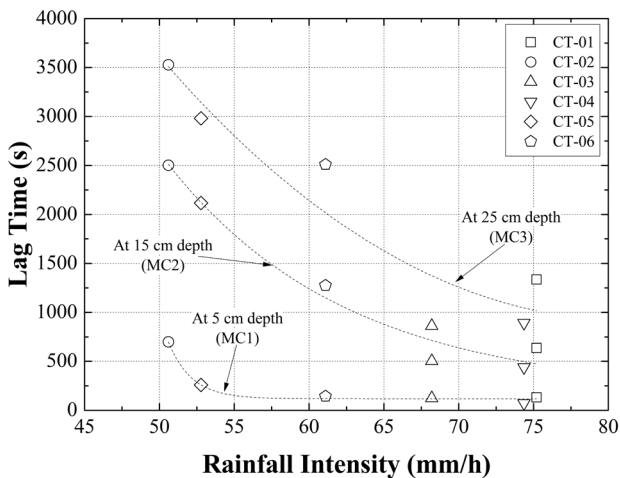


Figure 9 Rainfall intensity vs lag time measured by the MC sensors

4. Conclusions

In this study, and for simplicity, the infiltration process was analyzed in two stages. The first stage is when water enters into the soil, and the second one when the infiltrated water is redistributed within the soil profile after the cessation of the rainfall. Based on this assumption, the following conclusions are drawn:

- The initial water content measured by the sensors, before inducing the rainfall, is greater along the sand column as the depth of the column increases.

This suggests that water advances downward due to gravitational forces until equilibrium is reached.

- The time histories of moisture contents obtained at all depths (Figure 6) show the existence of a steady state infiltration. This response was captured independently of the initial water content and rainfall intensity of the sand column.
- The drainage process is related to the capillary barrier created at the soil-geotextile interface at the bottom of the sand column [21, 22]. In that sense, the residual water content measured by the bottom WC sensor was higher than those measured at depths of 5 and 15 cm.
- The elapsed time between rainfall initiation and the arrival of the wetting front at the different locations of the sand column (lag time) was strongly affected by the initial volumetric water content and rainfall intensity. However, from this study, it was not possible to conclude which of these parameters had the stronger influence on the infiltration process. More research is still needed to better understand and define this matter.
- Water movement throughout an unsaturated zone is commonly considered to be a one-dimensional flow in the downward direction. The results obtained from the sand column tests indicate that they can be used to determine the effects of initial volumetric water content and rainfall intensity on the water movement through unsaturated slopes and embankments.

5. Acknowledgments

The authors would like to thank the Geotechnical Laboratory of Tokyo University where the experimental work was performed.

6. References

1. N. Romano, B. Brunone, and A. Santini, "Numerical analysis of one-dimensional unsaturated flow in layered soils," *Adv. Water. Resour.*, vol. 21, no. 4, pp. 315-324, 1998.
2. V. Ravi and J. R. Williams, "Estimation of infiltration rate in the vadose zone: Compilation of simple mathematical models," United States Environmental Protection Agency (EPA), Tech. Rep. EPA/600/R-97/128a, Feb. 1998.
3. Y. Ma, S. Feng, D. Su, G. Gao, and Z. Huo, "Modeling water infiltration in a large layered soil column with a modified Green-Ampt model and HYDRUS-1D," *Computers and Electronics in Agriculture*, vol. 71, no. 1, pp. S40-S47, 2010.
4. K. Kamiya and S. Yamada, "An experimental study on pore-air behavior during water and seepage process in unsaturated soil," in *6th Int. Conf. on Unsaturated Soils*, Sydney, Australia, 2014, pp. 1131-1136.
5. M. A. Herrada, A. Gutierrez, and J. M. Montanero, "Modeling infiltration rates in a saturated/unsaturated soil under the free draining condition," *Journal of Hydrology*, vol. 515, pp. 10-15, 2014.

6. R. Srivastava and T. Jim, "Analytical solutions for one-dimensional, transient infiltration toward the water table in homogeneous layered soils," *Water Resour. Res.*, vol. 27, no. 5, pp. 753-762, 1991.
7. T. Zhan and C. Ng, "Analytical analysis of rainfall infiltration mechanism in unsaturated soils," *Int. J. Geomech.*, vol. 4, no. 4, pp. 273-284, 2004.
8. L. Z. Wu and L. M. Zhang, "Analytical solution to 1D coupled water infiltration and deformation in unsaturated soils," *Int. J. Numer. Anal. Met.*, vol. 33, no. 6, pp. 773-790, 2009.
9. G. F. Pinder and W. G. Gray, *Essentials of Multiphase Flow and Transport in Porous Media*, 1st ed. New Jersey, USA: Wiley, 2008.
10. D. V. Griffiths and N. Lu, "Unsaturated slope stability analysis with steady infiltration or evaporation using elasto-plastic finite elements," *Int. J. Numer. Anal. Met.*, vol. 29, no. 3, pp. 249-267, 2005.
11. T. Iryo and R. K. Rowe, "Numerical study of Infiltration into a soil-geotextile column," *Geosynth. Int.*, vol. 11, no. 5, pp. 377-389, 2004.
12. G. Siemens and R. J. Bathurst, "Numerical parametric investigation of infiltration in one- dimensional sand-geotextile columns," *Geotext. Geomembranes*, vol. 28, no. 5, pp. 460-474, 2010.
13. E. García, F. Oka, and S. Kimoto, "Numerical analysis of a one-dimensional infiltration problem in unsaturated soil by a seepage-deformation coupled method," *Int. J. Numer. Anal. Met.*, vol. 35, no. 5, pp. 544-568, 2011.
14. S. Kimoto, F. Oka, and E. García, "Numerical Simulation of the Rainfall Infiltration on Unsaturated Soil Slope Considering a Seepage Flow," *Geotech. Eng.*, vol. 44, no. 3, pp. 1-13, 2013.
15. A. C. Liakopoulos, "Transient flow through unsaturated porous media," Ph.D. dissertation, University of California, Berkeley, USA, 1964.
16. H. Yang, H. Rahardjo, B. Wibawa, and E. Leong, "A soil column apparatus for laboratory infiltration study," *Geotech. Test. J.*, vol. 27, no. 4, pp. 347-355, 2004.
17. R. J. Bathurst, A. F. Ho, and G. A. Siemens, "A column apparatus for investigation of 1-D unsaturated-saturated response of sand-geotextile systems," *Geotech. Test. J.*, vol. 30, no. 6, pp. 1-9, 2007.
18. ASTM International, *Standard Practice for Classification of Soils for Engineering Purposes (Unified Soil Classification System)*, Standard ASTM D2487, 2011.
19. M. van Genuchten, "A closed-form equation for predicting the hydraulic conductivity of unsaturated soils," *Soil. Sci. Soc. Am. J.*, vol. 44, no. 5, pp. 892-898, 1980.
20. E. García, "Function of Permeable Geosynthetics in Artificial Unsaturated Embankments Subjected to Rainfall Infiltration," M.S. thesis, University of Tokyo, Tokyo, Japan, 2005.
21. T. Iryo and R. K. Rowe, "On the Hydraulic behavior of unsaturated nonwoven geotextiles," *Geotext. Geomembranes*, vol. 21, no. 6, pp. 381-404, 2003.
22. H. Krisdani, H. Rahardjo, and E. Leong, "Experimental Study of 1-D Capillary Barrier Model using Geosynthetic Material as the Coarse-Grained Layer," in *4th Int. Conf. on Unsaturated Soils*, Carefree, USA, 2006, pp. 1683-1694.